

# Compact Wideband Passive and Active Component Chips for Radio Astronomy Instrumentation

H. Rashid<sup>1</sup>, D. Meledin<sup>1,2</sup>, V. Desmaris<sup>1,2</sup>, E. Sundin<sup>2</sup>, and V. Belitsky<sup>1,2</sup>

*Abstract*— In the 2SB receivers, the rejection ratio is determined among other factors by the performance of the quadrature hybrids. We have developed and fine-tuned components that intended to be used in the IF chain and meet the requirements for new generation of compact wideband 2SB receivers. We present here the design and characterization of three multi-section compact wideband 3 dB quadrature couplers (coupled line coupler – Lange coupler–coupled line coupler). Specifically, the miniaturized 3-section hybrid chip made using thin-film technology utilizes gold plated transmission lines and air bridges to connect the fingers of the Lange coupler (middle section) The hybrids were designed to have the amplitude and phase imbalance better than 0.6 dB and  $\pm 3^\circ$  respectively over a 3.5-12.5 GHz and 4-16 GHz frequency bands. Experimental verification of the assembly at 293 K and 4 K shows very good agreement between the measurements and simulations. Additionally, we demonstrate the suitability of the miniature hybrid chips, by implementing them in a balanced amplifier designed using a modular approach, which demonstrated promising results.

## I. INTRODUCTION

The demand for wideband millimeter-submillimeter wave multi-pixel receivers is continuously increasing. So far, only DSB multi-pixel heterodyne systems have been demonstrated [1]. Implementing of wideband sideband separating mixers into multi-pixel design is hindered however, by the fact that the number and the size of passive and active components (LNA) increases, which leads to unpractical receiver pixel footprint. A typical sideband separating receiver consists of among others, RF and IF quadrature hybrids, bias-Ts, isolators and low noise amplifiers, see Fig. 1. One of the key figures of merit in sideband separating receivers is the image rejection ratio, which is mainly dependent on the overall amplitude and phase impedance of the receiver chain [2]. This sets tough requirements on both the RF and IF quadrature hybrids.

In order to shrink the wideband receiver pixel footprint, compact and wideband passive and active device are required. One way to reduce the size is to use substrates with high dielectric constant and to integrate the bias-T with the wideband IF hybrid [2]. Furthermore, by using a balanced LNA topology [3] (employing the wideband IF hybrids) would yield a both compact and wideband LNA with sufficient return loss, which

practically removes the need for having an isolator in the receiver chain [2]. Hence, the importance of wideband quadrature hybrid with excellent amplitude and phase imbalance performance is vital [4-5]. This way, only two devices, an integrated 2SB mixer including bias-T followed by balanced IF LNA are required instead of four, which saves space considerably and would improve the performance. Furthermore, it is essential for integration and fabrication purpose that the circuits are planar.

To meet these goals, both compact wideband IF (one octave) and RF circuits has been developed and demonstrated [4-6]. Some of these wideband circuits have successfully been integrated into ALMA Band 5 receivers [6] or in the SEPIA receiver [7], which demonstrated image rejection ratios typically better than 15 dB, which is a significant improvement [6]. However, to meet the future demands of wideband radio astronomy receivers (IF bandwidth of two octaves or more), a new generation of circuit with bandwidth and enhanced performance have been designed.

In the next section, two compact wideband hybrids are presented, one operating at 3.5-12.5 GHz, and one at 4-16 GHz. Measurements of the manufactured circuits show exceptional performance at both room and cryogenic temperatures.

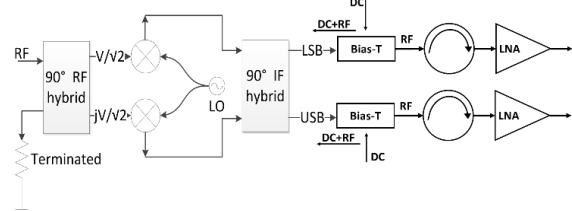


Fig. 1. Schematic of a sideband separating receiver

## II. HIGH PERFORMANCE WIDEBAND HYBRIDS

### A. Hybrid Topology

The requirement on the amplitude and phase imbalance was discussed in [5], where the maximum allowed imbalance was 0.6 dB and  $\pm 3^\circ$  respectively over one octave fractional bandwidth. However, future receivers require at least the same imbalance performance over two octaves or more. Hybrids employing single-section topologies cannot provide the required amplitude imbalance for bandwidths of greater than one octave at best [8, 9]. Therefore, multi-section layout must be used to meet the requirements upcoming

<sup>1</sup> Milliwave, Gothenburg, Sweden.

<sup>2</sup> Group for Advanced Receiver Development, Chalmers University of Technology, SE412 96, Gothenburg, Sweden.

wideband/multipixel receivers. A multi-section layout of three sections have been used here, since three sections is enough to meet the requirements, and the same time keep the circuit compact.

### B. Substrate selection

The possibility to use a substrate with reasonably high dielectric permittivity allows reaching compact design with minimum insertion loss; the latter depending on dielectric loss and conducting loss in the transmission lines. The miniature hybrid chip allows it to be integrated into virtually any sideband separating mixer, which is especially advantageous for multipixel receivers or low noise balanced amplifier layouts. Moreover, due to the multi-section design, it would be advantageous to use a substrate with high dielectric constant in order to minimize the overall chip dimensions. Therefore, Alumina substrate was selected as it exhibits excellent mechanical properties, low loss tangent, good thermal conductivity, and a dielectric constant of 9.6 at the design frequency.

### C. Three section hybrids

The proposed design employs a symmetrical three-section coupler. The even mode characteristic impedance for each stage of the multi-section coupler can be found in tables for a given equi-ripple across the band [10]. Two hybrids with different bandwidths were designed. The design procedure in both cases are the same. First step is to calculate the coupling coefficients of each section of the hybrid. The center section has always the highest coupling coefficient, while the adjacent sections are rather weakly coupled. Therefore, the first and the third sections are realized as a coupled line coupler structure whereas the middle section coupler employs a Lange coupler. Through these choices of couplers, the final structure becomes planar and the hybrid dimensions are completely determined by photolithography process. The miniaturized 3-section hybrid chip are made using thin-film technology, which utilizes gold plated transmission lines and air bridges to connect the fingers of the Lange coupler (middle section). A schematic of the three-section hybrid is illustrated in Fig. 2.

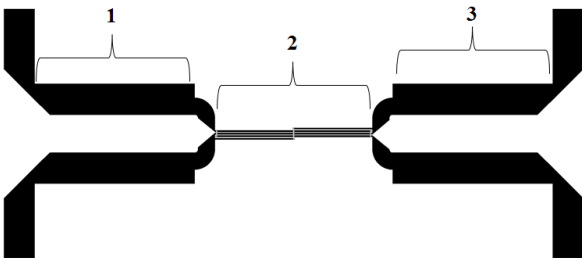


Fig. 2: The 3-section IF hybrid schematic, first and third sections are the coupled line couplers whereas the second section is the Lange coupler.

The initial dimensions for the multi-section coupler were calculated with Keysight ADS [10] LineCalc, using the coupling coefficients as described above. The complete hybrid structure was then optimized with Keysight Momentum [11]. The total length and width of the hybrid are 18.3 mm and 5 mm respectively. Fig.3 and Fig.4 shows the simulated performance

of the 3.5-12.5 GHz and 4-16 GHz hybrid with excellent amplitude imbalance performance. Moreover, by employing superconducting Nb lines as described in [12] the performance can be further improved by removing unwanted capacitive coupling if the Lange coupler.

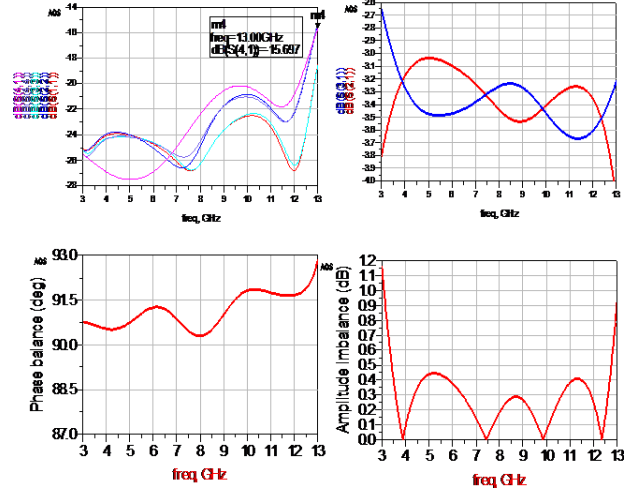


Fig. 3: Simulated performance of the 3.5-12.5 GHz hybrid. Top left: Reflection and isolation plot (dB). Top right: Through and coupled plot (dB). Bottom left: Phase balance (deg). Bottom right: Amplitude imbalance (dB).

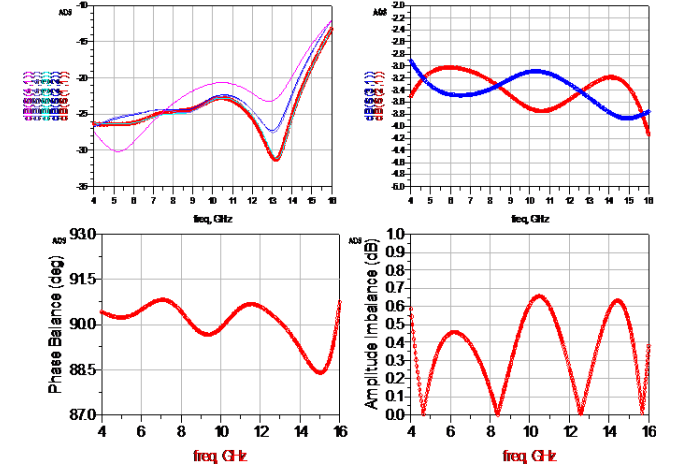


Fig. 4: Simulated performance of the 4-16 GHz hybrid. Top left: Reflection and isolation plot (dB). Top right: Through and coupled plot (dB). Bottom left: Phase balance (deg). Bottom right: Amplitude imbalance (dB).

## III. HYBRID PERFORMANCE

### A. Characterization setup

The fabricated chips were mounted in a housing featuring 4 K-type connectors, which was then installed in a cryostat for cooling down the samples down to 4K, using a close cycle machine. 4-port S-parameters measurements were carried out at room temperature (293 K) and at cryogenic temperatures (~4 K) using a Rohde&Schwarz ZVA40 vector network analyser (VNA). Owing to the lack of calibration standards at cryogenic temperatures, the S-parameters measurements at 4K were conducted using a special calibration procedure for cryogenic temperature, as described in details in [6]. The measured performance of the hybrids is shown in Fig. 5-9.

B. 3.5-12.5 GHz hybrid measured at 293 K

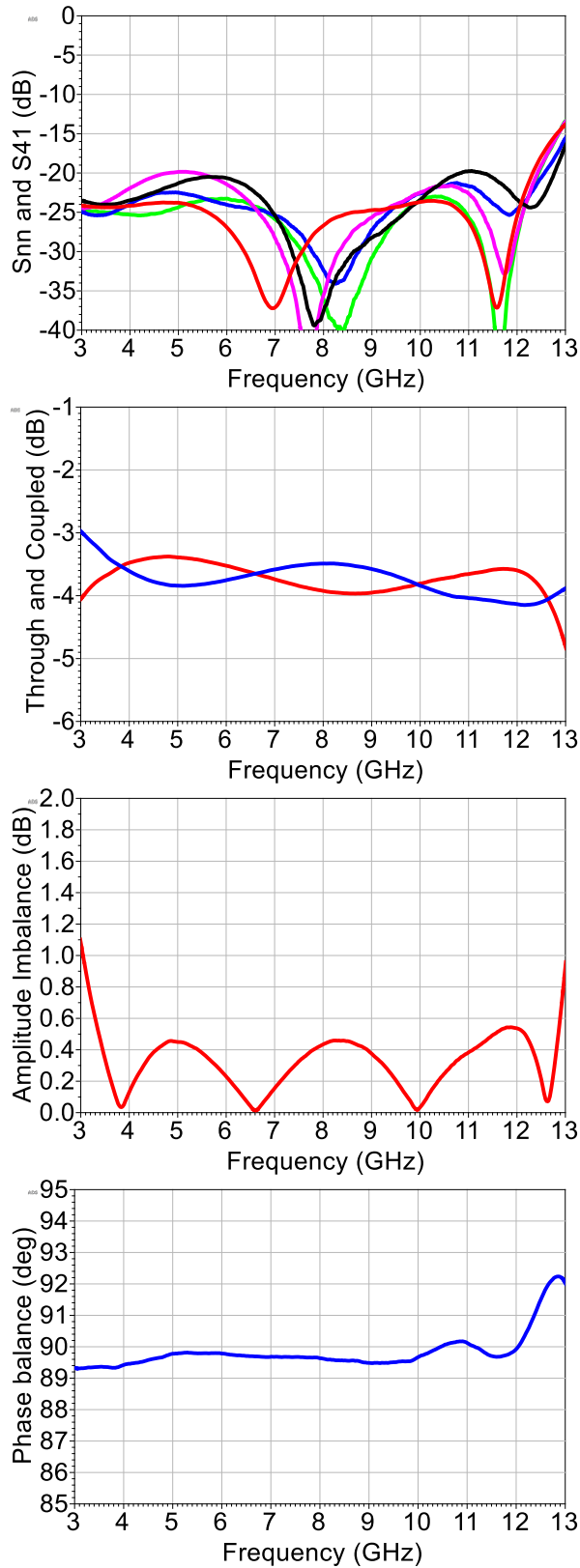


Fig. 5: Measured performance of the 3.5-12.5 GHz hybrid at 293 K. Figures from top to bottom represent: Reflection and isolation plot (dB); Though and coupled plot (dB); Amplitude imbalance (dB); Phase balance (deg.)

C. 3.5-12.5 GHz hybrid measured at 4 K

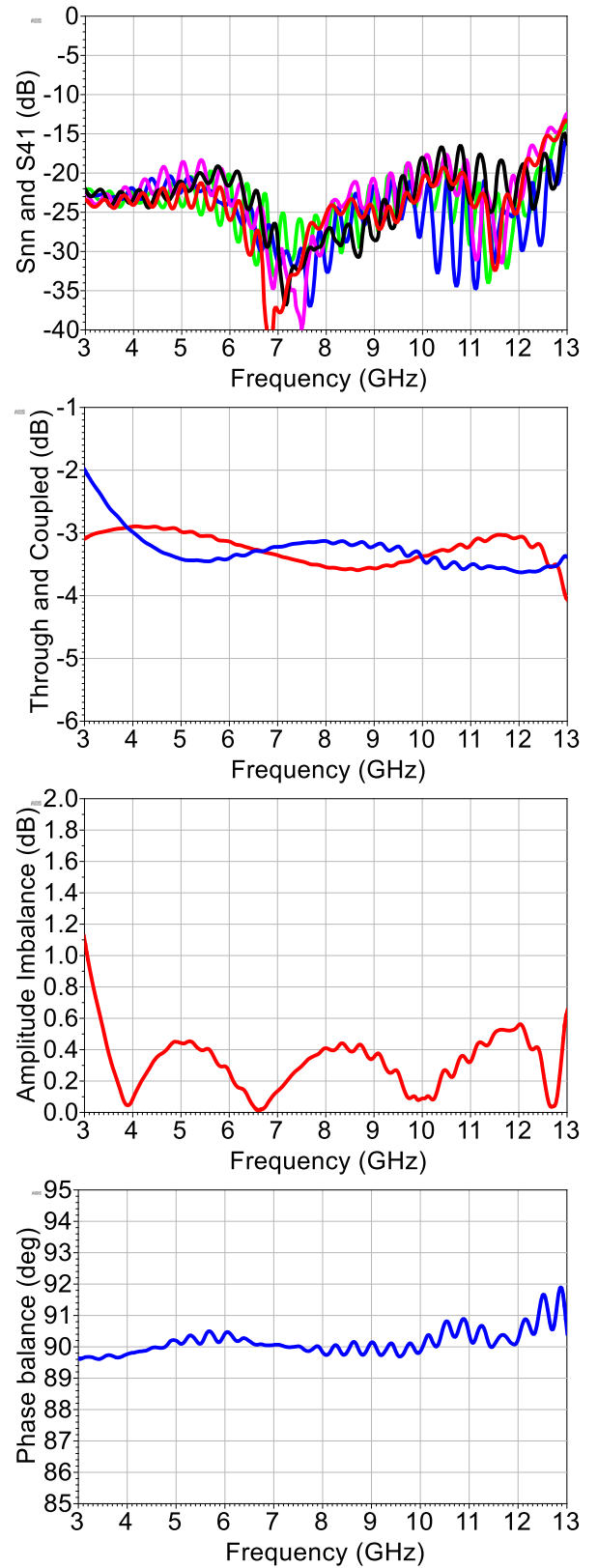


Fig. 6: Measured performance of the 3.5-12.5 GHz hybrid at 4 K. Figures from top to bottom represent: Reflection and isolation plot (dB); Though and coupled plot (dB); Amplitude imbalance (dB); Phase balance (deg.).

D. 4-16 GHz hybrid Measured at 293 K

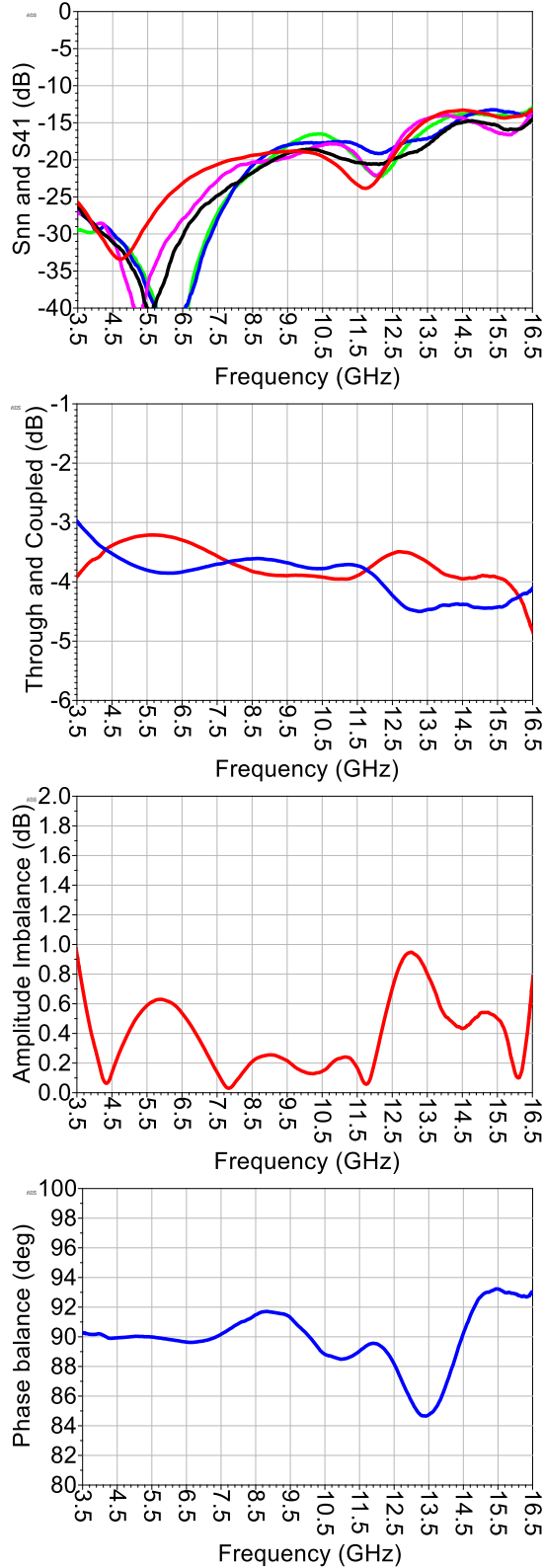


Fig. 7: Measured performance of the 4-16 GHz hybrid at 293 K. Figures from top to bottom represent: Reflection and isolation plot (dB); Though and coupled plot (dB); Amplitude imbalance (dB); Phase balance (deg.)

E. 4-16 GHz hybrid Measured at 293 K

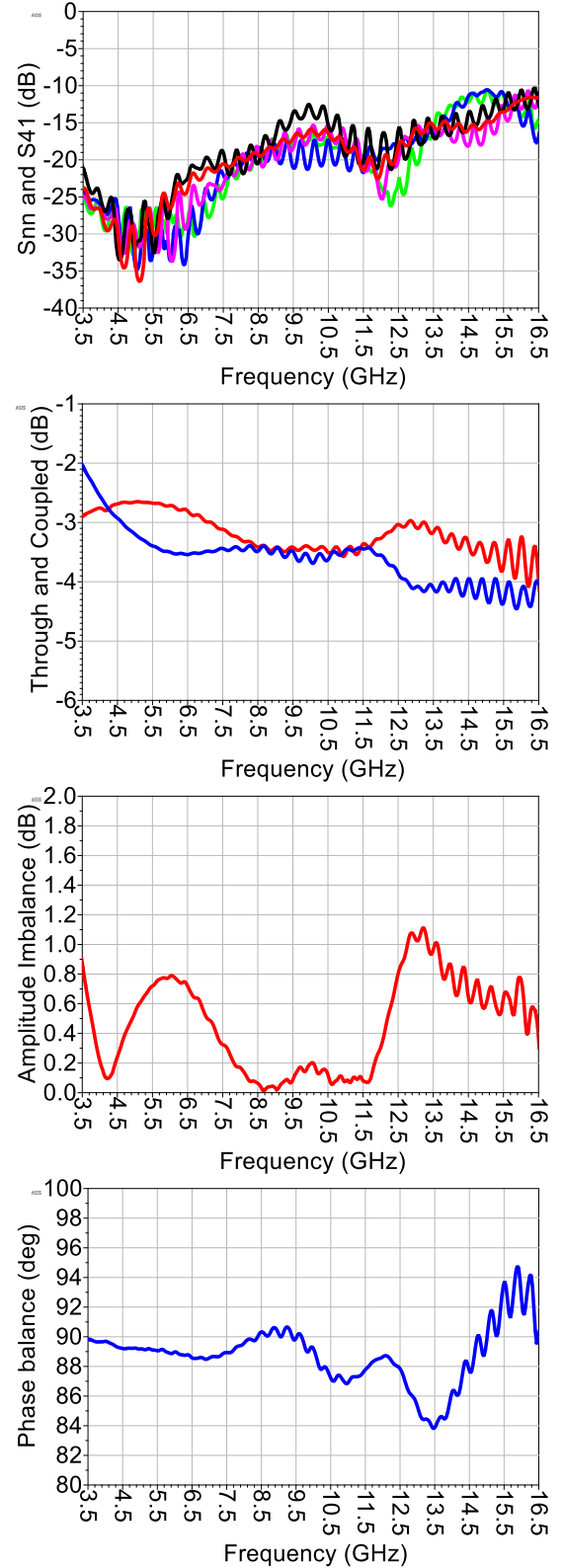


Fig. 8: Measured performance of the 4-16 GHz hybrid at 4 K. Figures from top to bottom represent: Reflection and isolation plot (dB); Though and coupled plot (dB); Amplitude imbalance (dB); Phase balance (deg.)

F. 4-12 GHz superconducting hybrid measured at 4K

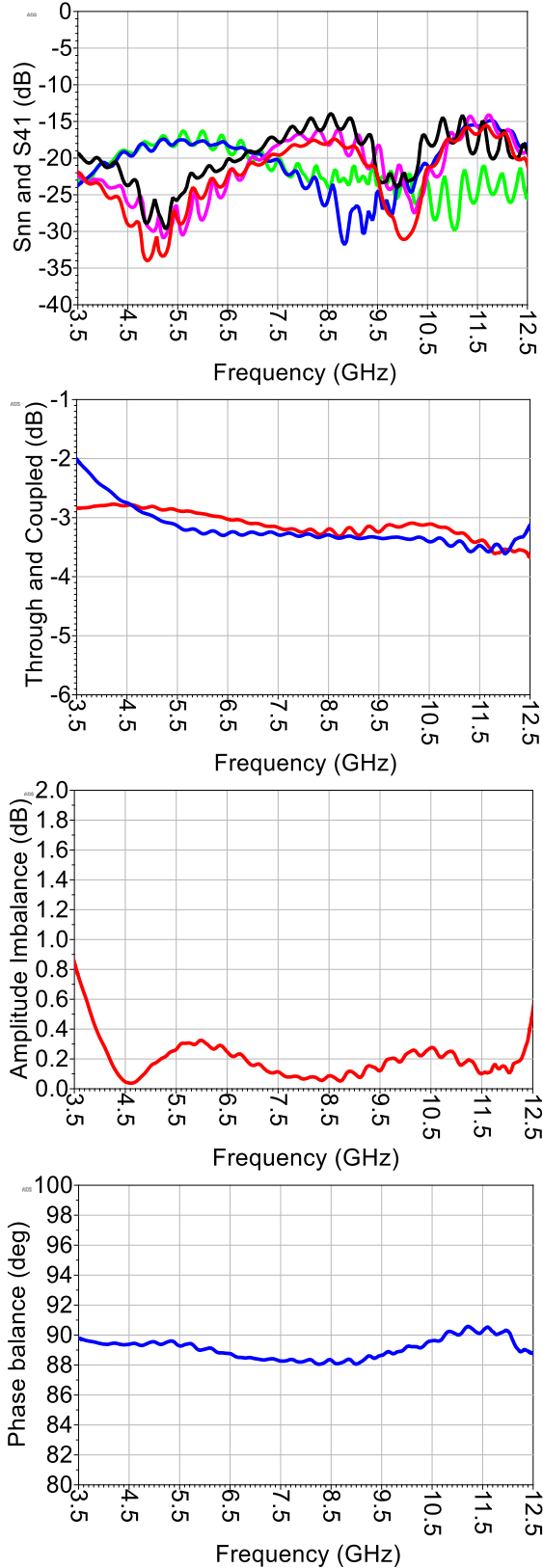


Fig. 9: Measured performance of the 4-12 GHz superconducting hybrid at 4 K. Figures from top to bottom represent: Reflection and isolation plot (dB); Through and coupled plot (dB); Amplitude imbalance (dB); Phase balance (deg.).

G. The hybrids' performance

Comparing Fig. 5 to 6, it can be seen that the amplitude and phase imbalance 3.5-12.5 GHz hybrid are not affected by the change in temperature, even though the insertion loss is clearly improved when the devices are operated at 4K, most likely due to the increase of conductivity of the metallic microstrip lines when cooling down the device.

Despite of a slight over-coupling, we observe a similar relative independence of the amplitude and phase imbalance as well as an improvement of the insertion loss for the 4-16 GHz hybrids, as shown on as shown on Fig. 7 and Fig. 8. However for this particular hybrid, we observe a discrepancy in return loss between the measurement results Fig. 7 and the simulation in Fig. 3 is probably due to due mounting or/and fabrication

The 4-12 GHz hybrid made of superconducting transmission lines shows measured 4-12 GHz hybrid with almost ideal performance and is very suitable for integration into 2SB THz receivers based on superconducting mixers.

IV. BALANCED AMPLIFIER CHARACTERIZATION

A. Practical implementation

An advantageous use of the miniaturize chips would be their implementation in balanced amplifiers, eventually used in the IF amplification chain of cryogenic receivers. Therefore, we constructed a modular balanced amplifier using 2 single end 4-16 GHz LNF-LNC4\_16B amplifiers from Low Noise Factory [13] and two wideband miniature 3dB 90 degrees hybrids: one 4-12 GHz hybrid at the input and one 4-16 GHz hybrid at the output (Fig. 10). Obviously, the modular approach is not optimum, since it introduced many interfaces and parasitics originating from the connection between the different elements of the amplifier. Yet it is a good test bed for evaluating the hybrids' performance.

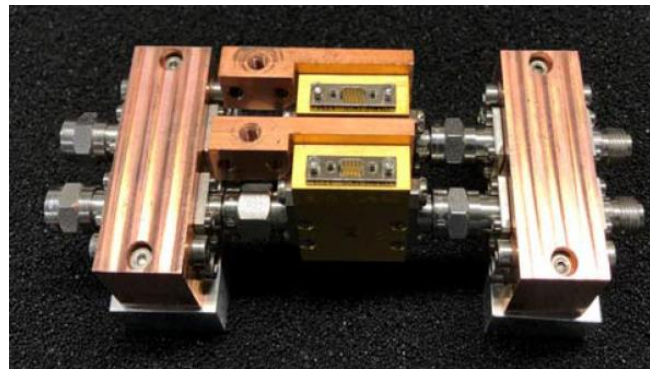


Fig. 10. Modular balanced amplifiers featuring two miniature hybrids and two single-end amplifiers.

B. Characterization setup

The noise performance of the LNAs were measured in a cryogenic system comprising a cryostat equipped with a 2-stage close cycle-machine, which allows cooling down to 4 K (Fig. 10). The noise temperature measurements were performed by the standard Y-factor technique and using the cold attenuator method similarly to [3], with an Agilent N4000A ENR noise

diode and an Agilent MXA N9020A spectrum analyzer with noise figure measurement option. The input and output reflection factors were measured after removal of the cold attenuator using a Rohde&Schwarz ZVA40, employing a specific calibration procedure described in [6] and biasing the individual amplifiers under the exact same conditions as during the noise measurements.

C. Characterization results

The noise temperature and gain of the balanced amplifier over the 4-12 GHz frequency band are presented in Fig. 11, whereas the input and output reflection factors are plotted in Fig 12.

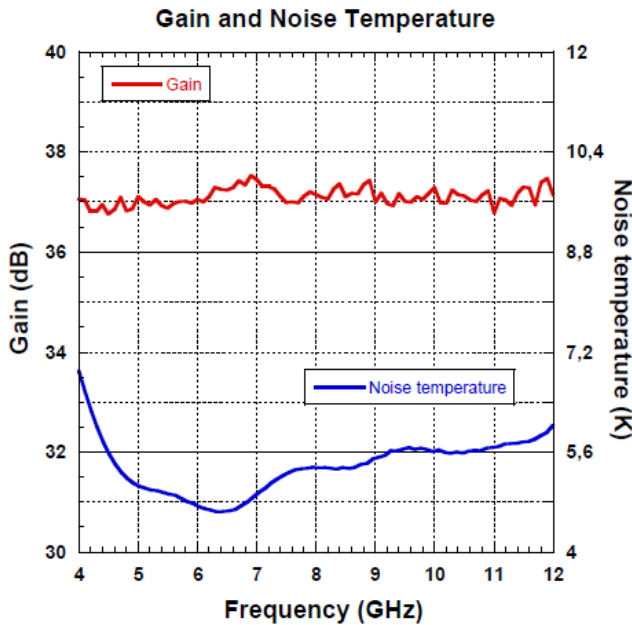


Fig. 11. Gain and Noise temperature of the Modular balanced amplifier.

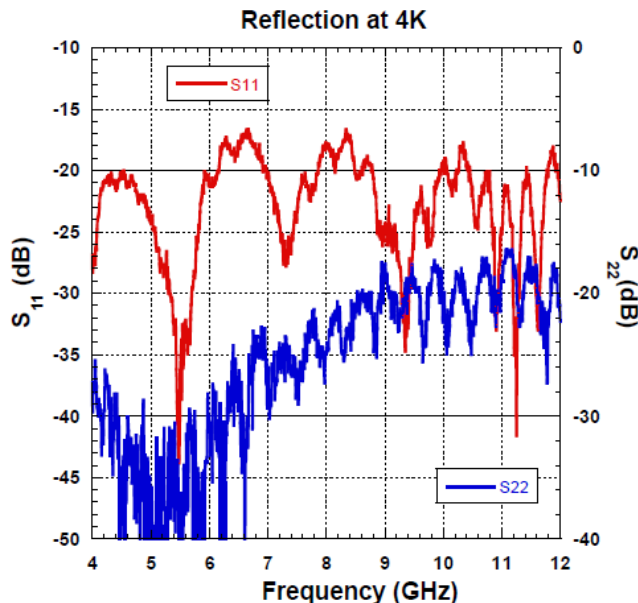


Fig. 12. Gain and Noise temperature of the Modular balanced amplifier.

The results show an improvement of about 5-7 dB in terms of return loss of the balanced amplifier as compared to the single-end amplifiers, yet without noticeable deterioration of the gain performance, which is consistent with our expectations. However, the noise temperature was raised by about 1K on average over the 4-12 GHz frequency range. This is likely to be ascribed to the inevitable parasitic effects introduced by the modular design with its different internal and external (SMA) interconnections and the fact that the hybrids used in this experiment are made of Gold transmission lines, which is not completely lossless even at cryogenic temperatures.

V. CONCLUSIONS

In this work, we report on the design and characterization of a 3.5-12.5 GHz and 4-16 GHz quadrature 3 dB directional couplers. The compact size of the hybrid chip allows it to be integrated into virtually any sideband separating (2SB) mixer operating at room temperature or cryogenic temperatures and is furthermore especially advantageous for multi-pixel 2SB receivers or balanced amplifier layouts.

The hybrid was fabricated using in-house thin-film technology on Alumina substrate and uses air bridges to inter-connect the fingers of the Lange coupler. The four-port S-parameters measurement showed very good agreement with the simulation results.

Furthermore, the good performance measured on a modular balanced amplifier constructed using the miniaturized hybrid chips let us to believe that with further integration of the chips in the amplifier designs even more broadband and compact IF LNAs could be realised for future use in radioastronomy receivers.

ACKNOWLEDGMENT

The authors would like to acknowledge Sven-Erik Ferm for his help with the fabrication of the mechanical fixtures to for the measurement tests.

The research leading to these results has received funding from the European Commission Seventh Framework Programme (FP/2007-2013) under grant agreement No 283393 (RadioNet3).

REFERENCES

- [1] C. E. Groppi and J. H. Kawamura, "Coherent Detector Arrays for Terahertz Astrophysics Applications," *Terahertz Science and Technology, IEEE Transactions on*, vol. 1, pp. 85-96, 2011.
- [2] I. Malo-Gomez, J. D. Gallego-Puyol, C. Diez-Gonzalez, I. Lopez-Fernandez, and C. Briso-Rodriguez, "Cryogenic Hybrid Coupler for Ultra-Low-Noise Radio Astronomy Balanced Amplifiers," *Microwave Theory and Techniques, IEEE Transactions on*, vol. 57, pp. 3239-3245, 2009
- [3] E. Sundin, A. Ermakov, V. Desmaris, H. Rashid, D. Meledin, M. Bylund and V. Belitsky, "Cryogenic IF Balanced LNAs Based on Superconducting Hybrids for Wideband 2SB THz Receivers", *Proceedings of the ISSTT2017*, Cologne, Germany, 2017.
- [4] H. Rashid, D. Meledin, V. Desmaris, and V. Belitsky, "Novel Waveguide 3 dB Hybrid With Improved Amplitude Imbalance," *Microwave and Wireless Components Letters, IEEE*, vol. 24, pp. 212-214, 2014.
- [5] H. Rashid, D. Meledin, V. Desmaris, A. Pavolotsky, and V. Belitsky, "Superconducting 4-8 GHz Hybrid Assembly for 2SB

- Cryogenic THz Receivers," *Terahertz Science and Technology, IEEE Transactions on*, vol. 4, pp. 193-200, 2014.
- [6] V. Belitsky *et al.*, "ALMA Band 5 receiver cartridge: Design, performance, and commissioning", *Astronomy and Astrophysics*, vol. 611, A68, 2018.
- [7] V. Belitsky *et al.*, "SEPIA – a new single pixel receiver at the APEX telescope", *Astronomy and Astrophysics*, vol. 612, A23, 2018.
- [8] B. Billade, H. Rashid, V. Desmaris, and V. Belitsky, "Superconducting 4 - 8 GHz IF Hybrid for Low Noise mm-Wave Sideband Separation SIS Receiver," *Microwave and Wireless Components Letters, IEEE*, vol. 22, pp. 589-591, 2012.
- [9] H. Rashid, P. Y. Aghdam, D. Meledin, V. Desmaris, and V. Belitsky, "Wideband Planar Hybrid With Ultralow Amplitude Imbalance," *IEEE Microwave and Wireless Components Letters*, vol. 27, pp. 230-232, 2017.
- [10] E. G. Cristal and L. Young, "Theory and Tables of Optimum Symmetrical TEM-Mode Coupled-Transmission-Line Directional Couplers," *Microwave Theory and Techniques, IEEE Transactions on*, vol. 13, pp. 544-558, 1965.
- [11] ADS. [www.keysight.com](http://www.keysight.com).
- [12] V. Belitsky *et al.*, "Superconducting microstrip line model studies at millimetre and sub-millimetre waves". *International Journal of Infrared and Millimeter Waves*. 27. Pp. 809-834, 2006
- [13] <https://www.lownoisefactory.com/products/cryogenic/4-16-ghz/>